Solvent Effects in Chemical Processes. Water-Assisted Proton Transfer Reaction of Pterin in Aqueous Environment†

Paula Jaramillo, Kaline Coutinho, and Sylvio Canuto*

Instituto de Física, Universidade de São Paulo, CP 66318, 05314-970, São Paulo, SP, Brazil

Received: April 20, 2009; Revised Manuscript Received: July 21, 2009

Pterins are members of a family of heterocyclic compounds present in a wide variety of biological systems and may exist in two forms, corresponding to an acid and a basic tautomer. In this work, the proton transfer reaction between these tautomeric forms was investigated in the gas phase and in aqueous solution. In gas phase, the intramolecular mechanism was carried out for the isolated pterin by quantum mechanical second-order Møller−Plesset perturbation theory (MP2/aug-cc-pVDZ) calculations and it indicates that the acid form is more stable than the basic form by −1.4 kcal/mol with a barrier of 34.2 kcal/mol with respect to the basic form. In aqueous solution, the role of the water molecules in the proton transfer reaction was analyzed in two separated parts, the direct participation of one water molecule in the reaction path, called water-assisted mechanism, and the complementary participation of the aqueous solvation. The water-assisted mechanism was carried out for one pterin-water cluster by quantum mechanical calculations and it indicates that the acid form is still more stable by −3.3 kcal/mol with a drastic reduction of 70% of the barrier. The bulk solution effect on the intramolecular and water-assisted mechanisms was included by free energy perturbation implemented on Monte Carlo simulations. The bulk water effect is found to be substantial and decisive when the reaction path involves the water-assisted mechanism. In this case, the free energy barrier is only 6.7 kcal/mol and the calculated relative Gibbs free energy for the two tautomers is −11.2 kcal/mol. This value is used to calculate the pK_a value of 8.2 ± 0.6 that is in excellent agreement with the experimental result of 7.9.

1. Introduction

Solvents are important and necessary ingredients in chemistry laboratories. As solvent changes molecular properties compared to the isolated molecule it is important to understand the solvent effects.[1] In recent years, much theoretical efforts have been devoted in this direction. The theoretical developments to understand and rationalize the role of solvents and of the liquid environment on molecular properties have been substantial.[2,3] Spectral and structural problems have been largely studied.[4] Some more development is still necessary to understand chemical reaction in solution. This is crucial in molecular biology, for instance, where several reactions necessary to create and sustain living systems can only occur in aqueous environment. Some recent studies indicate that the solvent is a direct participant[5] of the reaction process instead of a simple passive dielectric. In these cases, water-assisted and hydrogen bond wires[5] are essential for the efficiency of the reaction. This has important consequences in acid-basic proton transfer.[6] Analyzing chemical reaction in solution is a great theoretical effort necessitating the detailed inclusion of the solvent molecules and the accurate determination of the relative Gibbs free energies along the reaction process. In this work, we focus on this problem and study the proton transfer reaction for the acid−basic equilibrium of pterin in aqueous environment (see Figure 1). In addition, the accurate determination of the equilibrium constant and the corresponding pK_a value is also addressed to corroborate the validity of the numerical results in two different mechanisms, the direct intramolecular proton transfer (see Scheme 1) and water-assisted intermolecular proton transfer (see Scheme 2).

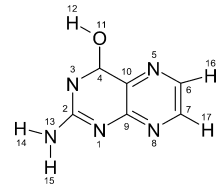

Figure 1. Schematic representation of the 2-aminopteridin-4(3H)-one pterin and the numerical labels.

SCHEME 1: Intramolecular Mechanism

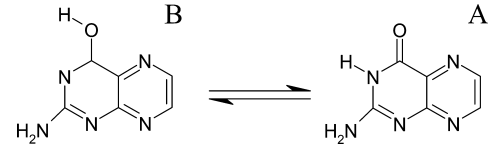

SCHEME 2: Water-Assisted Mechanism

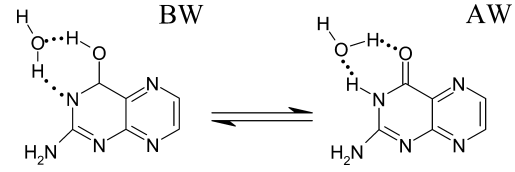

Pterins are members of a family of heterocyclic compounds present in biological systems and participating in important biological functions[7] including a primary role in photosynthetic electron transport. Pterins are also involved in different photochemical processes and have been found in photosensitive

† Part of the "Russell M. Pitzer Festschrift".

* To whom correspondence should be addressed. E-mail: canuto@if.usp.br. Fax: +55.11.3091-6745.

10.1021/jp903638n CCC: $40.75
Published on Web 09/14/2009

organs.[8] The absorption spectra of pterins were also studied to determine the mechanisms of coloration of pierid wings.[9] Some studies suggested that pterins might act as blue antennas in superior plants[10] and fungus.[11] Recently it has also been shown that it participates as sensitizers in photochemical reactions that induce DNA damage.[12] Thomas et al.[13] have investigated the efficiencies of $^1O_2$ production and the quenching of a class of pterins in aqueous solution. They have also reported[14] the fluorescence, absorption spectra, and the effects of substituents and pH.[15] For biological investigations, some pteridines have been synthesized and elucidated.[16] NMR spectrum of ^{15}N was also used to characterize the dominant tautomer in the equilibrium in aqueous solution of quinonoid tetrahydropterin.[17]

On the theoretical side, early studies have investigated geometries,[18] tautomeric, and protonation energy[19] at the ab initio level of dihydropterins. This latter also discussed the mechanism of enzymatic reduction.[19] Hartree−Fock calculations[20] were used to study the relative stability of the tautomers of dihydropterins and the interactions with the Moco cofactor. These studies suggest that the stability of the different tautomers of pteridines depend on the pH and solvation medium. Another work[21] has shown that the oxo form of pterin is more stable than the enol form and analysis of this tautomeric reaction served to elucidate a possible binding to dihydrofolate reductase, which is a target for anticancer drugs.[21] Docking methodology[22] was used to study the interactions with pteridine reductase of *Trypanosoma cruzy*. The optical properties of pterins have been studied[23] in the gas phase and solvent effects were included only at a simple level using continuum models.

To understand most of the biological activities of pterins, it is essential to have a better understanding of the tautomeric proton transfer reaction. Pterin may exist in two tautomeric forms (Scheme 1). Tautomeric reactions involve the interconversion between two chemical structures.[24] These structures can be converted into one another by a proton transfer passing through a transition state. Therefore, reliable quantum mechanical calculations[25] are necessary to provide the relative energy, or free energy, of the two stable forms and the transition state and hence an insight into the proton transfer and the equilibrium of the reaction. Normally, the equilibrium favors one form and it depends on several factors such as molecular structure, resonance, intramolecular hydrogen bonding with solvent molecules, polarity, temperature, and so forth. These factors should be considered in tautomeric equilibrium studies for calculating equilibrium constants,[25e] tautomeric energies,[19,20] stabilities of tautomers,[25d] solvent effects[5,25c,e] and so forth, as in several studies of equilibrium forms of keto-enol,[25a,e] thiol-thione[5g] and imino-amina.[25f]

Experimentally, it is known that the acid form of pterin is more stable in water and neutral pH.[17] Previous theoretical studies on the tautomeric stability obtained the same trend for similar compounds.[17,19] In the present work, we study the proton transfer reaction between the two tautomers of pterin (acid and basic) in the gas phase and in water solution. Quantum mechanical (QM) gas phase results are obtained at the second-order MP2 level. Single point calculations using the high-level CCSD(T) coupled-cluster method were also made to verify the reliability of the results. Two possible reaction pathways were studied and compared. One is the direct intramolecular proton transfer where the hydrogen atom of the hydroxyl of the basic form migrates to bond itself to the neighbor nitrogen, N3, (see Figure 1). This mechanism takes place without explicit participation of solvent water in the process. The other reaction path is the intermolecular water-assisted proton transfer where the hydrogen atom of the hydroxyl of the basic form of pterin migrates to bind on the water molecule and concomitantly a hydrogen of this water molecule migrates to bind to the nitrogen N3 of the pterin (see Scheme 2). For these two mechanisms, additionally, the effects of the aqueous environment were investigated. Using Monte Carlo (MC) simulation and thermodynamic perturbation theory,[26] as used before,[5g] the variations of free energies, the equilibrium constant and the pK_a for the tautomeric reaction were calculated. Because of the close proximity of the donor and acceptor of the hydrogen atom in the transfer process, we will only consider the participation of one explicit water molecule. To corroborate the results, these are used in the calculation of the pK_a value and excellent values are obtained using different QM levels of calculation.

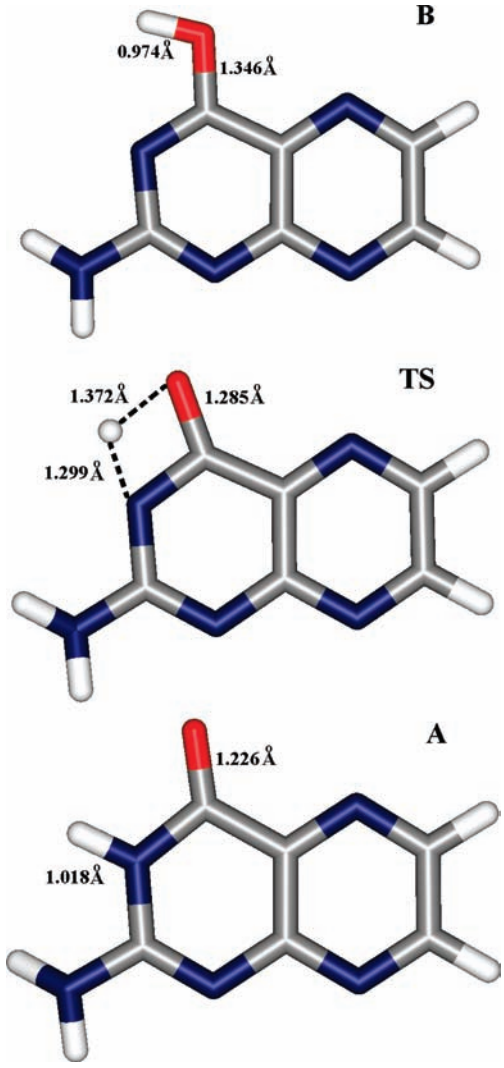

Figure 2. Optimized structures of pterin in the intramolecular process of tautomerization. B is the basic form, TS is the transition state, and A is the acid form. The distances shown were obtained from the MP2/aug-cc-pVDZ geometry optimization.

2. Computational Details

2.1. Quantum Mechanics Calculations. The geometrical structures for 2-aminopteridin-4(3H)-one pterin in basic form (B), in the acid form (A), and the transition state (TS) were optimized using the density-functional theory (DFT) methods B3LYP[27]/6-31+G(d,p) and PBE[28]/6-31+G(d,p) and the second-order MP2[29]/aug-cc-pVDZ level of theory. The structures obtained with MP2 are shown in Figure 2, and it describes the

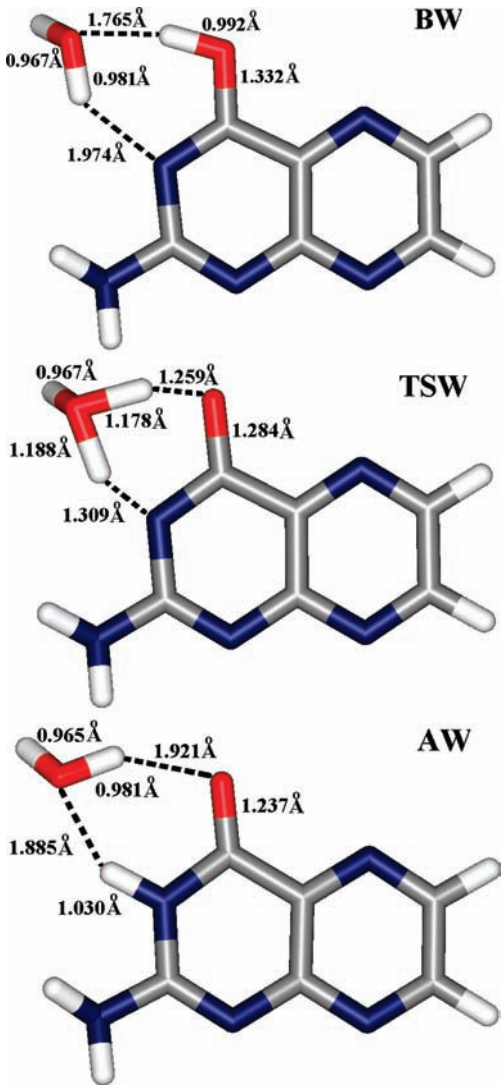

Figure 3. Optimized structures of pterin in the water-assisted process of tautomerization. BW is the basic form, TSW is the transition state, and AW is the acid form. All optimized with one water molecule. The distances shown were obtained from the MP2/aug-cc-pVDZ geometry optimization.

intramolecular mechanism of the proton transfer shown in Scheme 1. The structures for the water-assisted mechanism of the proton transfer shown in Scheme 2 were also optimized in gas phase with the same level of calculations. These are shown in Figure 3 and correspond to (i) the basic form (BW), (ii) the acid form (AW), and (iii) the transition state (TSW) all bonded with one water molecule.

The nature of the stationary points was confirmed by calculating vibrational frequencies using the harmonic approximation. A true minimum was verified for the four structures: A, B, AW and BW. The transition states, TS and TSW, were also confirmed with only one imaginary frequency. The frequency calculations also provided the free energy and relevant contributions for the energy such as zero-point vibrational and thermal corrections at room temperature.

The solvent effects on the geometrical properties were also analyzed using geometry optimization of the corresponding structures (shown in Figures 2 and 3) with the Onsager continuum model[30] for the aqueous solvent with B3LYP/6-31+G(d,p) level of calculation as implemented in the Gaussian 03 program.[31]

TABLE 1: Lennard-Jones Parameter of the OPLS Force Field[32]

atoms	ε in kcal/mol	σ in Å
C2	0.066	3.500
C6, C7, C9 and C10	0.070	3.550
H16 and H17	0.030	2.420
H12, H14 and H15	0.000	0.000
N1, N3, N5, N8 and N13	0.170	3.250
	0.066 (basic)	3.500 (basic)
C4	0.105 (transition state)	3.705 (transition state)
	0.105 (acid)	3.705 (acid)
	0.170 (basic)	3.120 (basic)
O11	0.190 (transition state)[a]	3.040 (transition state)[a]
	0.210 (acid)	2.960 (acid)

[a] The parameter of the O11 in the transition state was defined as an average between the parameter of the same atom in the basic and acid forms.

2.2. Monte Carlo Simulation. The MC simulations were performed using standard procedure for Metropolis sampling technique applied for liquid system of rigid molecules in the NPT ensemble.[32] In all simulations, one solute molecule (A, B, TS, AW, BW, and TSW) was embedded in 500 water molecules at a pressure of 1 atm and a temperature of 298.15 K. The molecules were kept rigid during the simulation. For the transition state structures (TS and TSW), the parameters of the intramolecular potential are not available and to calculate the differential free energy of solvation a comparative analysis should be done for the three structures (B, TS and A or BW, TW and AW). Thus we only use the intermolecular interactions in the simulation but the intramolecular part of the interactions is taken care by the quantum mechanical calculations. The intermolecular interactions were described by the Lennard-Jones (LJ) plus Coulomb potential with three parameters for each atom i (ε_i, σ_i, and q_i). For the water molecules the SPC/E[33] potential and geometry were used. For all solute molecules, the geometries were optimized with B3LYP/6-31+G(d,p) and the potential interaction was described by the Lennard-Jones parameters of the OPLS force field[34] (see Table 1) and the atomic charges were calculated using the fitting of the electrostatic potential with the CHELPG procedure implemented in the Gaussian 03 program[31] at the MP2/aug-cc-pVDZ level including the solute polarization with the iterative QM/MM procedure, as used before.[35] In this iterative procedure, a set of atomic charges of the solute is calculated in gas phase, then a simulation is performed. In the equilibrium stage of 3.75×10^7 MC steps, an average solvent electrostatic configuration (ASEC)[36] is generated (with 100 statistically uncorrelated configuration and 250 water molecules) and a QM MP2/aug-cc-pVDZ calculation is performed to generate a new set of atomic charges of the solute embedded in the electrostatic field of the solvent. Using this new set of atomic charges, a new simulation is performed and this procedure is repeated until a convergence is obtained for the dipole moment of the solute. At that point, the charge distribution of the solute is in electrostatic equilibrium with the solvent distribution and vice versa.

The free energy perturbation theory[26] (FEP) was used to study the solvent effect in the proton transfer reaction of pterin in aqueous solution through the intramolecular and water-assisted mechanisms. The variation of the Gibbs free energy between two states I and J in solution is calculated by the equation

$$\Delta G_{solv}(I \rightarrow J) = -k_B T \ln\langle \exp[-(\Delta H)/k_B T] \rangle_I \qquad (1)$$

SCHEME 3: Thermodynamic Cycle

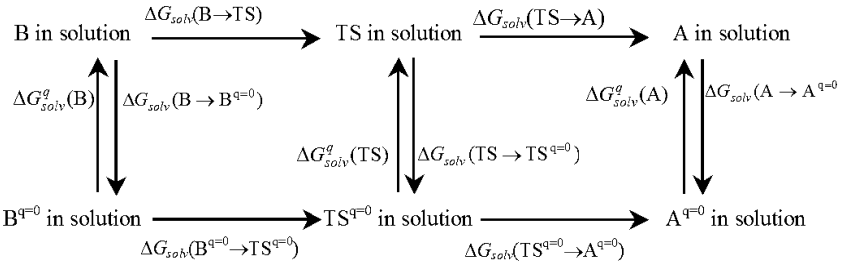

where ΔH is the variation of the enthalpy of the two states sampled in the configurations of state I in solution. Although the eq 1 is exact, the convergence of the relative free energy is slow if I and J are very dissimilar. Therefore, it is usually necessary to perform a series of intermediate simulations that gradually mutate the state I into state J using a coupling parameter λ. This parameter varies between 0 and 1 and scales the geometry, the coulomb charges, and the LJ parameters when changing from I to J

$$H(\lambda) = H_I - \lambda(H_J - H_I) \quad (2)$$

In the case of the proton transfer reaction of pterin in solution, the state I was considered as the basic form (B in the intramolecular mechanism and BW in the water-assisted mechanism) and the state J was considered as the acid form (A and AW), in ΔG_{solv}(B→A) and ΔG_{solv}(BW→AW). A similar procedure is adopted when calculating the reaction barrier, ΔG_{solv}(B→TS) and ΔG_{solv}(BW→TSW).

Therefore, the direct calculation of ΔG_{solv}(B→A) (shown in Scheme 1) using FEP through a direct mutation of B into A requires a very large series of simulation. However, using a simple thermodynamic cycle the calculation of ΔG_{solv}(B→A) can be performed using the difference of the free energy of solvation,[37] ΔG_{solv}(B→A) = ΔG_{gas}(B→A) + ΔG_{solv}(A) − ΔG_{solv}(B). Then, the free energy of solvation of each species, ΔG_{solv}(X), is calculated using the vanishing approach,[37] that is, the solute is completely vanished from the solution and the free energy of annihilation is calculated, ΔG_{solv}(X) = −ΔG_{solv}(X→0). In addition, this free energy of annihilation is calculated in two parts. First, the Coulomb term of the potential interaction is made to vanish. Next, the LJ term is made to vanish also. Following these ideas, we propose here an alternative and nonphysical thermodynamic cycle (see Scheme 3) to calculate the variation of the Gibbs free energy of the basic−acid reaction process, ΔG_{solv}(B→A) using the vanishing approach.[37] But, instead of completely vanishing the solute X in the solution and calculate the free energy of solvation, here only the Coulomb term of the interacting potential is made to vanish, ΔG_{solv}(X→X$^{q=0}$). After that, the remaining part is calculated with a direct mutation between the species with non-Coulomb term of interaction, X$^{q=0}$. This second part is proposed here, because the geometries (Figures 2 and 3) and the LJ potential parameters (Table 1) of the solvated molecule are similar (essentially only three atoms change, N3, O11, and H12) and the direct mutation from B$^{q=0}$ to TS$^{q=0}$ and next to A$^{q=0}$ can be done with a small series of simulations. Therefore, for the system studied here, the thermodynamic cycle proposed in Scheme 3 involves fewer simulations than the traditional thermodynamic cycle with the complete annihilation of the solute in the solvent environment.

In Scheme 3, the mutation of the basic form B into the acid form A of the pterin in solution was divided in two subcycles, ΔG_{solv}(B→A) = ΔG_{solv}(B→TS) − ΔG_{solv}(A→TS). Then

$$\Delta G_{solv}(X \rightarrow TS) = \Delta G_{solv}(X^{q=0} \rightarrow TS^{q=0}) + \Delta\Delta G^{q}_{solv}(X \rightarrow TS) \quad (3)$$

where

$$\Delta\Delta G^{q}_{solv}(X \rightarrow TS) = \Delta G^{q}_{solv}(TS) - \Delta G^{q}_{solv}(X) \quad (4)$$

is the differential electrostatic solvation between the TS and X = B or A. This term is given by the difference of the Coulomb term of the free energy of solvation that is calculated with the vanishing approach ΔG^{q}_{solv}(X) = −ΔG_{solv}(X→X$^{q=0}$), where X = B, TS, and A.

To calculate the electrostatic term of the free energy of solvation, ΔG^{q}_{solv}(X), the Coulomb potential was made to vanish by scaling to zero the atomic charges of each solute X. The scale factors were λ = 1.0, 0.9, 0.8, 0.7, 0.6, 0.5, 0.3, and 0.0. Using the double-wide sampling[37a] in a simulation performed with λ_i (example λ_i = 0.9), the charges of the solute were perturbed simultaneously for λ_{i-1} and λ_{i+1} (where λ_{i-1} = 1.0 and λ_{i+1} = 0.8). Therefore, only four simulations were performed with λ = 0.9, 0.7, 0.5 and 0.3 to vanish the Coulomb potential of the solute. After that, the solute molecules became nonphysical systems with the same geometries and LJ potential but without Coulombic term. They were called as B$^{q=0}$, TS$^{q=0}$, A$^{q=0}$ (and BW$^{q=0}$, TSW$^{q=0}$ and AW$^{q=0}$). The next step was the calculation of ΔG_{solv}(X$^{q=0}$→TS$^{q=0}$), where a direct mutation was performed changing the Cartesian coordinates (x, y, z) and the LJ parameters, ε and σ, from the basic B$^{q=0}$ and acid forms A$^{q=0}$ to the transition state TS$^{q=0}$. The scale factors were λ = 1.00, 0.75, 0.50, 0.25, and 0.00. Using the double-wide sampling again, only two simulations were performed, with λ = 0.75 and 0.25. Note that only the intermolecular part of the ΔG_{solv}(X$^{q=0}$→TS$^{q=0}$) is calculated in the simulation, ΔG^{inter}_{solv}(X$^{q=0}$→TS$^{q=0}$). Then, it is necessary to add the intramolecular part, ΔG^{intra}_{solv}(X$^{q=0}$→TS$^{q=0}$) that was obtained from the optimized geometries in the QM calculations for the isolated solute molecules, ΔG^{intra}_{solv}(X$^{q=0}$→TS$^{q=0}$) = ΔG(X→TS). Therefore

$$\Delta G_{solv}(X^{q=0} \rightarrow TS^{q=0}) = \Delta G^{inter}_{solv}(X^{q=0} \rightarrow TS^{q=0}) + \Delta G^{intra}_{solv}(X \rightarrow TS) \quad (5)$$

These calculated values will be presented and discussed in the next section.

In total, 16 simulations were performed using FEP with double-wide sampling: three times four simulations to vanish

TABLE 2: Geometric Parameters for the Tautomers and the Transition State Optimized for the Proton Transfer of Pterin in the Intramolecular and Water-Assisted Mechanisms, Using MP2/aug-cc-pVdz Level (in Parentheses the B3LYP/6-31+G(d,p) Results with the Onsager Continuum Solvent Model); Distances in Angstroms and Angles in Degrees

geometric parameters intramolecular mechanism	basic B	transition TS	acid A
dihedral C4–C10–C9–N1	0.0 (0.0)	1.5 (0.0)	1.6 (0.0)
angle O11–C4–N3	119.4 (119.2)	107.0 (106.4)	121.0 (120.6)
angle C4–N3–C2	116.5 (117.1)	122.0 (121.8)	124.6 (124.4)[123.0][a]
bond C2–N3	1.383 (1.373)	1.369 (1.366)	1.382 (1.382) [1.400][b]
bond N1–C2	1.328 (1.329)	1.320 (1.327)	1.308 (1.312) [1.340][b]
bond N3–C4	1.315 (1.308)	1.348 (1.349)	1.408 (1.404) [1.340][b]
bond C4–O11	1.346 (1.335)	1.285 (1.281)	1.226 (1.220)
bond C4–C10	1.442 (1.440)	1.438 (1.436)	1.485 (1.478) [1.420][b]

geometric parameters water-assisted mechanism	basic BW	transition TSW	acid AW
dihedral C4–C10–C9–N1	–0.1 (0.2)	–1.9 (0.1)	2.0 (–0.2)
dihedral C2–N3–C4–O11	–180.0 (–179.7)	–180.0 (–179.3)	–174.9 (–179.3)
angle O11–C4–N3	120.7 (120.7)	119.6 (119.4)	121.3 (120.7)
angle C4–N3–C2	117.0 (117.4)	120.4 (120.3)	123.9 (123.9)
bond C2–N3	1.381 (1.373)	1.372 (1.370)	1.377 (1.376)
bond N1–C2	1.326 (1.328)	1.315 (1.324)	1.305 (1.311)
bond N3–C4	1.325 (1.320)	1.355 (1.358)	1.392 (1.395)
bond C4–O11	1.332 (1.319)	1.284 (1.276)	1.237 (1.229)
bond C4–C10	1.446 (1.447)	1.453 (1.456)	1.474 (1.474)

[a] Experimental value taken from ref 39a. [b] Experimental values taken from ref 39b.

the Coulomb term of the solute−solvent interaction and in addition two times two simulations for the direct mutation of the transition state to the basic and acid tautomers with only the LJ term of the solute−solvent interaction. Each simulation starts with the last configuration of the previous simulation, and it consists of a thermalization stage of 15.0×10^6 MC steps, followed by an equilibrium stage of 75.0×10^6 MC step. The statistical error of the free energy calculated by FEP was estimated for each simulation considering half of the minimum-maximum difference of the accumulative values of the free energy in the last 50.0×10^6 MC step of the simulation. These were all summed to have the final total value. All the simulations, using standard MC and double-wide FEP, were performed with the DICE program.[38]

After calculating the variation of the Gibbs free energy in the tautomeric proton transfer process in solution, the equilibrium constant (or tautomerization constant) K_T can be obtained by

$$\Delta G_{solv}(B \rightarrow A) = -k_B T \ln(K_T) \quad (6)$$

From this, the pK_a value can be obtained simply by

$$pK_a = \log(K_T) = \frac{-\Delta G_{solv}(B \rightarrow A)}{2.3 k_B T} \quad (7)$$

The calculated pK_a for this tautomeric reaction in both mechanisms considered in this work, intramolecular and water-assisted, will be reported and discussed.

3. Results and Discussions

3.1. Geometry and Free Energy of Reaction for Isolated Molecules. The structures optimized with MP2/aug-cc-pVDZ for the isolated solutes for both intramolecular and water-assisted proton transfer mechanisms are shown in Figures 2 and 3. Only the structural parameters with appreciable changes in the proton transfer reaction are summarized in Table 2. For comparison, in Table 2 the values for the geometry optimized using the Onsager continuum model for the water solvent are shown in parentheses. Experimentally only the X-ray diffraction[39] of the principal ring of pterin is known. These experimental values are also shown in Table 2. The experimental C2−N3 distance of 1.400 Å and the calculated values of 1.383 and 1.382 Å for the basic and acid tautomer respectively are in good agreement. In the solvent, the distance slightly changes to 1.373 Å for the basic form and is unchanged in the acid form. The experimental angle C4−N3−C2 is 123° and the calculated value for the acid tautomer is 125° both for the isolated molecule and with the solvent model. Also, in agreement with experimental information obtained from X-ray the ring is calculated to be planar. The tautomeric reaction induces changes in the bond lengths and bond angles and these are involved in the formation of the N−H and C═O bonds of the acid tautomer (see Figure 2). When the reaction goes from B, passing in TS to reach A, the angle O11−C4−N3 in the intramolecular mechanism changes from 119° in B to 107° in TS and 121° in A both for the isolated molecule and in the solvent. The bond length C4−O11 decreases from 1.346 Å in B to 1.285 Å in TS to 1.226 Å in A for the isolated molecule and 1.335 Å in B, 1.281 Å in TS, and 1.220 Å in A in the solvent. This intramolecular mechanism proceeds through a three-center transition state with an imaginary frequency of 1841i cm^{-1}, computed at the MP2/aug-cc-pVDZ. The nuclear displacement associated with this normal mode displays a concerted mechanism in which the O−H bond (in B) is broken and the N−H (in A) is formed.

The values of the geometrical properties shown in Table 2 clearly suggest that the solvent effect in the geometry is very small and is negligible using the Onsager continuum model for this reaction process. The changes in the geometry presented by the solvent are small and essentially the same as the changes obtained when these isolated molecules are optimized with different DFT methods (B3LYP and PBE with 6-31+G(d,p)). Therefore, it seems that the structures obtained for the proton

TABLE 3: The Electronic and Total Energies, $\Delta E^{Ele}(X)$ and $\Delta E^{Total}(X)$, and the Gibbs Free Energy $G(X)$ of the Solute X Computed for the Proton Transfer of Pterin in the Intramolecular Mechanisms[a]

energy intramolecular mechanism	basic X = B	transition state X = TS	acid X = A
	B3LYP/6-31 + G(d,p)		
$\Delta E^{Ele}(X)$	−580.683494	−580.624766	−580.686212
$\Delta E^{Total}(X)$	−580.553178	−580.499777	−580.555438
$G(X)$	−580.596575	−580.542684	−580.598997
$\Delta E^{Ele}(B\rightarrow X)$	0.00	36.85 (36.68)	−1.71 (−3.97)
$\Delta E^{Total}(B\rightarrow X)$	0.00	33.51	−1.42
$\Delta G(B\rightarrow X)$	0.00	33.82	−1.52 −1.73[b]
$\Delta G(X\rightarrow TS)$	33.82	0.00	35.34 29.99[b]
	MP2/aug-cc-pVDZ		
$\Delta E^{Ele}(X)$	−579.158360	−579.098500	−579.160362
$\Delta E^{Total}(X)$	−579.028319	−578.972922	−579.030184
$G(X)$	−579.071194	−579.016713	−579.073389
$\Delta E^{Ele}(B\rightarrow X)$	0.00	37.56 38.60[c]	−1.26 −1.26[c]
$\Delta E^{Total}(B\rightarrow X)$	0.00	34.76	−1.17
$\Delta G(B\rightarrow X)$	0.00	34.19	−1.38
$\Delta G(X\rightarrow TS)$	34.19	0.00	35.57

[a] Absolute values are in au and relative values in kcal/mol. In parentheses, the electronic energy obtained with geometry optimized with the Onsager continuum solvent model. [b] Values obtained with PBE/6-31+G(d,p). [c] Values obtained with CCSD(T)/aug-cc-pVDZ.

transfer reaction of the pterin in the intramolecular mechanism are insensitive to the particular theoretical or solvent model.

In the same way, the water-assisted mechanism does not change appreciably the structure of the pterin ring. But the presence of one explicit water molecule induces small changes in the planarity of AW. BW is planar but AW presents a small deviation from the planarity. The dihedral angle C2−N3−C4−O11 in BW is −180° and in AW it is −175° for the isolated molecule and −180° for both BW and AW in the solvent. The formation of the C═O bond is evident in the AW form with a bond length C4−O11 of 1.237 Å for the isolated molecule and 1.229 Å in the solvent. In this mechanism, the water molecule initially forms a hydrogen bond with the basic form (BW) (see Figure 3) with the water molecule acting as an acceptor of hydrogen. Further interaction leads to the transition state with an imaginary frequency of 1534i cm^{-1} in which a concerted motion of the hydrogen of the O−H group and the hydrogen of the water molecule takes place. The acid form, AW, is then generated as a hydrogen-bonded complex. Similar to the direct mechanism, in this water-assisted mechanism the changes in the geometry presented by the solvent are small and essentially the same as the changes obtained when these isolated molecules are optimized with different DFT methods (B3LYP and PBE with 6-31+G(d,p)). For both mechanisms, the equilibrium and transition state structures are relatively rigid and have only a small dependence with the theoretical level of calculation or the solvent model.

The relative and absolute energies and Gibbs free energies are listed in Tables 3 and 4 for the intramolecular and water-assisted mechanisms, respectively. For comparison, in these tables are also presented the values for the relative electronic energy using the Onsager continuum model for the water solvent and also the values for the relative Gibbs free energy for different DFT methods. The acid tautomers are more stable than the basic tautomers in all levels of theory considered (see Tables 3 and 4). Thus the tautomeric reaction was considered from the basic to the acid forms. For the intramolecular mechanism, we calculated a barrier of $\Delta G(B\rightarrow TS) = 33.82$ kcal/mol after correcting for zero-point energy vibrations and thermal correction for the energy, enthalpy, and Gibbs free energy with the B3LYP/6-31+G(d,p) level. The acid−base relative free energy was calculated as $\Delta G(B\rightarrow A) = -1.52$ and −1.73 kcal/mol with B3LYP/6-31+G(d,p) and PBE/6-31+G(d,p), respectively. Aiming at obtaining more reliable results we reoptimized the three structures and calculated the energies and free energies with more systematic electron correlation effects using MP2/aug-cc-pVDZ level. The results now show a free energy barrier of 34.19 kcal/mol and an acid−base difference of −1.26 kcal/mol. Although the barrier is now slightly higher than at the B3LYP level, the sign and the magnitude of the relative free energy did not change, showing that the acid tautomer is still more stable than the basic form.

To verify the role of higher-order electron correlation effects, single point calculations were also made at the CCSD(T)/aug-cc-pVDZ levels. Comparing the relative electronic energies with respect to the basic form, $\Delta E^{Ele}(B\rightarrow X)$, it can be noted that the energy, 38.60 kcal/mol, of the TS is now slightly increased by ∼1 kcal/mol and for the acid form it is the same, −1.26 kcal/mol, as that obtained using the MP2 level. This clearly suggests that the contribution of high-order electron correlation terms essentially cancel and the MP2 and CCSD(T) models give the same value for the electronic energy in gas phase. The MP2 results will then be taken as our reference value in the gas phase both in the direct and in the water-assisted mechanisms. In the water-assisted mechanisms with the inclusion of one water molecule, the calculated free energy barrier at the MP2 level is 10.37 kcal/mol and the acid−base difference is −3.25 kcal/mol. Figure 4 summarizes these results.

The water-assisted mechanism decreases the free energy barrier by 23.82 kcal/mol leading to a value of 10.37 kcal/mol instead of 34.19 kcal/mol in the intramolecular mechanism. Thus the presence of one explicit solvent water molecule favors the acid−base proton transfer and the free energy calculated for this process is −3.25 kcal/mol (Table 4). Both mechanisms indicate that for the isolated molecule with or without explicit water the acid tautomers (A and AW) are favored and the tautomeric equilibrium is shifted to the acid form, in agreement with experiment.

TABLE 4: The Electronic and Total Energies, $\Delta E^{Ele}(X)$ and $\Delta E^{Total}(X)$, and the Gibbs Free Energy $G(X)$ of the Solute X Computed for the Proton Transfer of Pterin in the Water-Assisted Mechanisms[a]

energy water-assisted mechanism	basic X = BW	transition state X = TSW	acid X = AW
	B3LYP/6-31+G(d,p)		
$\Delta E^{Ele}(X)$	−657.133423	−657.114338	−657.139298
$\Delta E^{Total}(X)$	−656.975184	−656.963029	−656.981007
$G(X)$	−657.024152	−657.009680	−657.030583
$\Delta E^{Ele}(BW\rightarrow X)$	0.00	11.98 (11.70)	−3.69 (−3.63)
$\Delta E^{Total}(BW\rightarrow X)$	0.00	7.63	−3.65
$\Delta G(BW\rightarrow X)$	0.00	9.08	−4.04 −3.57[b]
$\Delta G(X\rightarrow TSW)$	9.08	0.00	13.12 8.25[b]
	MP2/aug-cc-pVDZ		
$\Delta E^{Ele}(X)$	−655.436499	−655.414542	−655.441000
$\Delta E^{Total}(X)$	−655.278533	−655.263183	−655.282910
$G(X)$	−655.327634	−655.311101	−655.332815
$\Delta E^{Ele}(BW\rightarrow X)$	0.00	13.78	−2.82
$\Delta E^{Total}(BW\rightarrow X)$	0.00	9.63	−2.75
$\Delta G(BW\rightarrow X)$	0.00	10.37	−3.25
$\Delta G(X\rightarrow TSW)$	10.37	0.00	13.62

[a] Absolute values are in au and relative values in kcal/mol. In parentheses, the electronic energy obtained with the geometry optimized with Onsager continuum solvent model. [b] Values obtained with PBE/6-31+G(d,p).

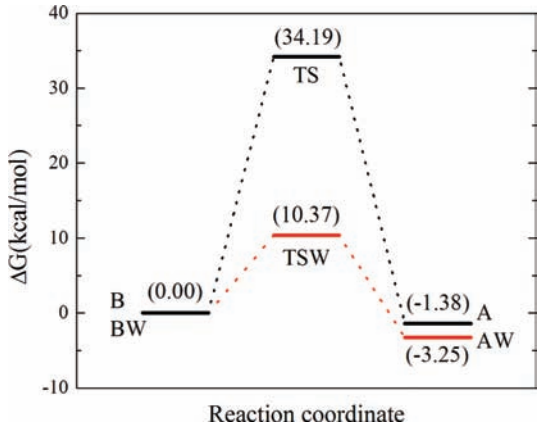

Figure 4. Schematic free energy profile for both tautomerization processes, intramolecular (isolated pterin) and water-assisted (one pterin and one water). All values were obtained with MP2/aug-cc-pVDZ level of calculation (see Tables 3 and 4).

TABLE 5: Computed Dipole Moment (μ in Debye) in the Isolated Gas Phase and after Solute Polarization in Aqueous Solution (See Text)[a]

intramolecular mechanism	basic B	transition state TS	acid A
μ (gas phase)	1.53	2.21	3.68
μ (in water)	2.83	3.14	5.50
water-assisted mechanism	basic BW	transition state TSW	acid AW
μ (gas phase)	1.59	1.91	2.40
μ (in water)	2.92	3.04	4.16

[a] All results were obtained at the MP2/aug-cc-pVDZ level.

3.2. Proton Transfer Reaction in Aqueous Solution. Now we consider the solvent effects of the bulk in the proton transfer reaction. These are made using MC simulations of pterin in aqueous environment. An important aspect to be considered is the solute polarization by the solvent. Solute polarization is a topic of central concern and has been included using different procedures.[40] The solute polarization here is the change in the electrostatic moments of a reference molecule as a consequence of the electric field provided by the solvent. To account for this, we used an iterative procedure that electrostatically equilibrates the solute in the solvent environment.[35] In the water-assisted mechanism, we consider one additional water molecule as part of the solute, as shown in Scheme 2 and Figure 3. The polarizations of these "solute" molecules A, TS, B, AW, TSW, and BW are given in Table 5. The gas phase dipole moment of the acid tautomer, considered here as A, at the MP2/aug-cc-pVDZ level is 3.68 D, increasing to 5.50 D in the water environment, an increase of ca. 50%. The acid tautomers A and AW show greater dipole moments than the basic tautomers, thus showing that in aqueous solution the acid form interacts more strongly with water and the solvent plays an important role in the increase of the stabilization of the acid form. Differently from the direct mechanism, in the water-assisted mechanism an additional water molecule is included in the process along with the bare pterin solute, so that the dipole moments shown in the Table 5 for the AW, TSW, and BW are for the pterin-water complex.

The variation of the free energy of the tautomeric process was calculated using the thermodynamic cycle described in Scheme 3. Initially, the Coulomb term of the potential of the solute molecule is annihilated (meaning that the Coulomb term of the intermolecular potential of the solute X goes to zero: $X\rightarrow X^{q=0}$) in solution, computing the $\Delta G_{solv}(X\rightarrow X^{q=0})$ using FEP described in eq 1. For each solute (B, TS, and A in the intramolecular mechanism and BW, TSW, and AW in the water-assisted mechanism), four simulations using the double-wide sampling were performed to make the Coulomb term of the solute X gradually disappear. The results of the $\Delta G_{solv}(X\rightarrow X^{q=0})$ are summarized in Table 6. For the intramolecular mechanism, the electrostatic contribution for the free energy of solvation for the basic form ($\Delta G^{q}_{solv}(B)$) is −26.81 kcal/mol, for the transition state ($\Delta G^{q}_{solv}(TS)$) it is −29.13 kcal/mol and for the acid form ($\Delta G^{q}_{solv}(A)$) it is −42.36 kcal/mol. Therefore the electrostatic interaction with the solvent stabilizes these three structures differently. Comparing to the basic form, the aqueous environment stabilizes the transition state by −2.32 kcal/mol and the acid form by −15.55 kcal/mol. These reflect the large difference in the dipole moments of the structures (see Table 5). After calculating this electrostatic term of the differential

TABLE 6: Coulomb Contribution for the Gibbs Free Energy of Solvation of the Two Tautomers and the Transition State Computed for the Proton Transfer of Pterin in the Intramolecular and Water-Assisted Mechanisms in Aqueous Solution at 298 K and 1 atm[a]

intramolecular mechanism		relative Gibbs free energy (kcal/mol)		
λ_i in q	λ_j in q	X = B	X = TS	X = A
1.0	0.9	6.35	6.75	9.32
0.9	0.8	5.28	5.61	8.12
0.8	0.7	4.41	4.72	6.99
0.7	0.6	3.59	3.77	5.72
0.6	0.5	2.57	3.11	4.38
0.5	0.3	3.10	3.68	5.32
0.3	0.0	1.51	1.49	2.51
$\Delta G_{solv}(X \rightarrow X^{q=0})$		26.81	29.13	42.36
$\Delta G^{q}_{solv}(X)$		−26.81	−29.13	−42.36
$\Delta\Delta G^{q}_{solv}(B \rightarrow X)$		0.00	−2.32	−15.55
$\Delta\Delta G^{q}_{solv}(X \rightarrow TS)$		−2.32	0.00	13.23
water-assisted mechanism		relative Gibbs free energy (kcal/mol)		
λ_i in q	λ_j in q	X = BW	X = TSW	X = AW
1.0	0.9	6.85	7.55	8.69
0.9	0.8	6.00	6.41	7.41
0.8	0.7	4.87	5.22	6.03
0.7	0.6	3.99	4.22	4.98
0.6	0.5	2.92	3.34	3.68
0.5	0.3	3.77	4.29	5.00
0.3	0.0	1.95	1.90	1.84
$\Delta G_{solv}(X \rightarrow X^{q=0})$		30.35	32.93	37.63
$\Delta G^{q}_{solv}(X)$		−30.35	−32.93	−37.63
$\Delta\Delta G^{q}_{solv}(BW \rightarrow X)$		0.00	−2.58	−7.28
$\Delta\Delta G^{q}_{solv}(X \rightarrow TSW)$		−2.58	0.00	4.70

[a] Results obtained from thermodynamic perturbation. See text.

free energy of solvation, the remaining term of the differential solvation was calculated by the direct mutation of the geometry and the van der Waals interactions of the structures without electrostatic interactions but only LJ parameters ($\Delta G_{solv}(TS^{q=0} \rightarrow B^{q=0})$ and $\Delta G_{solv}(TS^{q=0} \rightarrow A^{q=0})$). These results are given in Table 7. The direct mutation from the nonelectrostatic transition state ($TS^{q=0}$) to the nonelectrostatic basic form ($B^{q=0}$) gives a variation of free energy of 34.87 kcal/mol. Out of this, 0.68 kcal/mol is obtained from the intermolecular interaction calculated with the FEP simulations and 34.19 kcal/mol from the intramolecular interaction calculated with QM at the MP2/aug-cc-pVDZ level. For the direct mutation from $TS^{q=0}$ to the nonelectrostatic acid form ($A^{q=0}$) the calculated value is 35.68 kcal/mol, where 0.11 kcal/mol is obtained from the intermolecular interaction and 35.57 kcal/mol form the intramolecular interaction calculated with the same QM level. Therefore, the mutation from $B^{q=0}$ to $A^{q=0}$ that is given by $\Delta G_{solv}(B^{q=0} \rightarrow A^{q=0}) = -\Delta G_{solv}(TS^{q=0} \rightarrow B^{q=0}) + \Delta G_{solv}(TS^{q=0} \rightarrow A^{q=0})$ is −0.81 kcal/mol. To verify possible dependence on the QM approximation adopted, we have also used DFT methods and noted that these results are stable. For instance, changing the QM level of calculations to B3LYP and PBE with 6-31+G(d,p) basis set, this last value changes to −0.95 and −1.16 kcal/mol, respectively. Additionally, using the values of Tables 6 and 7 and the eqs 3, 4, and , the total differential free energy of solvation from the basic to the transition state and to the acid forms, ($\Delta G_{solv}(B \rightarrow TS)$ and $\Delta G_{solv}(B \rightarrow A)$), were calculated as 32.55 and −16.36 kcal/mol, respectively. All these values are summarized in Table 8. The final values show that the water environment stabilizes the transition state by −1.64 kcal/mol, changing the barrier free energy from 34.19 kcal/mol for the isolated molecules to 32.55 kcal/mol for the solvated situation. As for the acid tautomer it is stabilized by −14.98 kcal/mol, changing the relative free energy from −1.38 to −16.36 kcal/mol.

For the water-assisted mechanism, the situation is similar but the water environment stabilizes more the transition state by −3.70 kcal/mol, changing the barrier free energy from 10.37 kcal/mol for the isolated molecules to 6.67 kcal/mol for the solvated situation. The acid tautomer is stabilized by −7.96 kcal/mol, changing the relative free energy from −3.25 to −11.21 kcal/mol. Therefore, the differential free energy of solvation between the basic−acid tautomers is −11.21 kcal/mol, where −7.28 kcal/mol originates in the electrostatic term and −3.93 kcal/mol is from the remaining terms due to geometry change and van der Waals interaction.

Figure 5 summarizes the results including the effect of the aqueous environment in the proton transfer in both mechanisms. It also shows that the activation free energy is considerably lower in the water-assisted mechanism. The free energy barrier of 32.55 kcal/mol in the intramolecular mechanism is reduced to only 6.67 kcal/mol in the water-assisted mechanism in aqueous solution. It shows that the direct participation of the water molecule in the reaction and the water bulk effect decreases the barrier of 25.88 kcal/mol, increasing the reaction velocity. An opposite effect of the water was observed in the stabilization of the acid tautomer. It is more stable than the basic tautomer by 16.36 kcal/mol in the intramolecular mechanism and it is reduced to 11.21 kcal/mol in the water-assisted mechanism in solution; it is a destabilization of 5.15 kcal/mol.

Table 8 summarizes the free energy barrier and the variation of the Gibbs free energy between the basic−acid form of pterin in the intramolecular and water-assisted mechanisms, using QM calculations for the isolated solutes and free energy perturbation in Monte Carlo simulations for the solute in aqueous solution. The two effects of the solvent in the tautomeric reaction can be separately analyzed, the direct participation of one water molecule in the proton transfer reaction, comparing the results $\Delta G(B \rightarrow X)$ of isolated solutes in both mechanisms, and the bulk effect of water in the proton transfer, comparing the $\Delta G(B \rightarrow X)$ with $\Delta G_{solv}(B \rightarrow X)$ in both mechanisms. The most important effect of the direct participation of water in the reaction is observed in the decreasing of ca. 24 kcal/mol in the barrier (changing the barrier from 34.19 kcal/mol in the intramolecular mechanism to 10.37 kcal/mol in the water-assisted mechanism). In turn, the most important effect of the aqueous environment is observed in the increase of ca. 15 kcal/mol in the stabilization of the acid form (changing the relative stabilization of −1.38 kcal/mol in the intramolecular mechanism in gas phase to −16.36 kcal/mol in the same mechanism in aqueous solution). Adding these two effects of water in the reaction, our best results show a free energy barrier of 6.67 kcal/mol with a relative Gibbs free energy of −11.21 kcal/mol stabilizing the acid tautomer of the pterin in aqueous solution.

3.3. Determination of pK_a. An important verification to properly corroborate the reliability of the theoretical results for the proton transfer considered here is provided by the determination of pK_a. As seen in eqs 6 and 7 the pK_a value can be obtained directly from the free energy of tautomerization. It can be obtained as the difference of the free energy of the tautomerization process in solution, $\Delta G_{solv}(B \rightarrow A)$ for both mechanisms considered here using the electrostatic term of the free energy of solvation of the two tautomeric forms ($\Delta G^{q}_{solv}(B)$ and $\Delta G^{q}_{solv}(A)$ or $\Delta\Delta G^{q}_{solv}(B \rightarrow A)$), given in Table 6 and the direct mutation of the fictitious tautomeric form without electrostatic but only LJ interactions, ($\Delta G_{solv}(B^{q=0} \rightarrow A^{q=0})$), given

TABLE 7: Lennard-Jones Contribution for the Gibbs Free Energy of Interconversion of the Two Tautomers of Pterin into the Transition State Computed for the Intramolecular and Water-Assisted Mechanisms of Proton Transfer in Aqueous Solution at 298 K and 1 atm[a]

intramolecular mechanism		relative Gibbs free energy (kcal/mol)	
λ_i in ε, σ and (x, y, z) with $q = 0$	λ_j in ε, σ and (x, y, z) with $q = 0$	X = B	X = A
1.00	0.75	0.17	0.02
0.75	0.50	0.16	0.02
0.50	0.25	0.18	0.03
0.25	0.00	0.17	0.04
$\Delta G^{inter}_{solv}(X^{q=0} \rightarrow TS^{q=0})$		0.68	0.11
$\Delta G^{intra}_{solv}(X \rightarrow TS)^b$		34.19 (33.82)	35.57 (35.34)
$\Delta G_{solv}(X^{q=0} \rightarrow TS^{q=0})^c$		34.87 (34.50)	35.68 (35.45)
$\Delta G_{solv}(B^{q=0} \rightarrow X^{q=0})$		0.00	−0.81 (−0.95, −1.16[d])
water-assisted mechanism		**relative Gibbs free energy (kcal/mol)**	
λ_i in ε, σ and (x, y, z) with $q = 0$	λ_j in ε, σ and (x, y, z) with $q = 0$	X = BW	X = AW
1.00	0.75	−0.32	−0.14
0.75	0.50	−0.32	−0.16
0.50	0.25	−0.24	−0.07
0.25	0.00	−0.24	−0.07
$\Delta G^{inter}_{solv}(X^{q=0} \rightarrow TSW^{q=0})$		−1.12	−0.44
$\Delta G^{intra}_{solv}(X \rightarrow TSW)^e$		10.37 (9.08)	13.62 (13.12)
$\Delta G_{solv}(X^{q=0} \rightarrow TSW^{q=0})^c$		9.25 (7.96)	13.18 (12.68)
$\Delta G_{solv}(BW^{q=0} \rightarrow X^{q=0})$		0.00	−3.93 (−4.72, −4.25[d])

[a] Results obtained from thermodynamic perturbation theory and quantum mechanics calculations with MP2/aug-cc-pVDZ (in parentheses results obtained with B3LYP/6-31+G(d,p)). See text. [b] Values obtained from Table 3: $\Delta G^{intra}_{solv}(X \rightarrow TS) = G(X \rightarrow TS)$. [c] $\Delta G_{solv} = \Delta G^{int\ er}_{solv} + \Delta G^{intra}_{solv}$, see eq 5. [d] Values obtained with PBE/6-31+G(d,p). [e] Values obtained from Table 4: $\Delta G^{int\ ra}_{solv}(X \rightarrow TSW) = G(X \rightarrow TSW)$.

TABLE 8: Summary for the Gibbs Free Energy for the Intramolecular and Water-Assisted Mechanisms of Proton Transfer in Aqueous Solution at 298 K and 1 atm Used Thermodynamic Perturbation and Quantum Calculations with MP2/aug-cc-pVDZ (In Parentheses Results Obtained with B3LYP/6-31+G(d,p))

intramolecular mechanism	relative Gibbs free energy (kcal/mol) X = TS	X = A
	Isolated Molecules	
ΔG(B→X)	34.19 (33.82)	−1.38 (−1.52, −1.73[a])
pK_a		1.0 (1.1, 1.3[a])
	In Aqueous Solution	
$\Delta\Delta G^{q}_{solv}$(B→X)	−2.32	−15.55
$\Delta G_{solv}(B^{q=0} \rightarrow X^{q=0})$	34.87 (34.50)	−0.81 (−0.95, −1.16[a])
ΔG_{solv}(B→X)	32.55 (32.18)	−16.36 ± 0.80 (−16.50, −16.71[a])
pK_a		12.0 ± 0.6 (12.1, 12.3[a])
water-assisted mechanism	**relative Gibbs free energy (kcal/mol) X = TSW**	**X = AW**
	Isolated Molecules	
ΔG(B→X)	10.37 (9.08)	−3.25 (−4.04, −3.57[a])
pK_a		2.4 (3.0, 2.6[a])
	In Aqueous Solution	
$\Delta\Delta G^{q}_{solv}$(BW→X)	−2.58	−7.28
$\Delta G_{solv}(BW^{q=0} \rightarrow X^{q=0})$	9.25 (7.96)	−3.93 (−4.72, −4.25[a])
ΔG_{solv}(BW→X)	6.67 (5.38)	−11.21 ± 0.70 (−12.00, −11.53[a])
pK_a		8.2 ± 0.6 (8.8, 8.5[a])
experimental[14a] pK_a		7.9

[a] Values obtained with PBE/6-31+G(d,p).

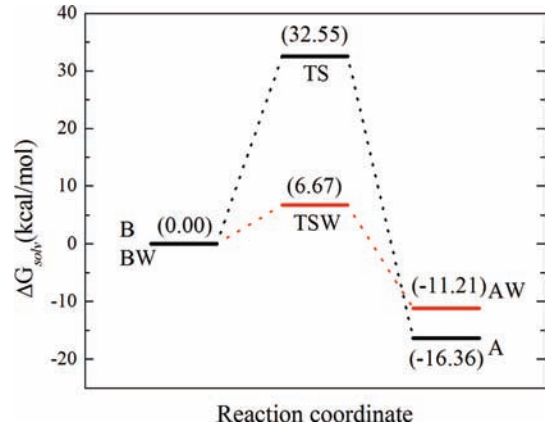

Figure 5. Schematic free energy profile for both tautomerization processes in solution, intramolecular and water-assisted. All values were obtained with MP2/aug-cc-pVDZ level of calculation (see Tables 6 and 7).

in Table 7. The quantities involved in eqs 3, 4, and 5 were calculated and were discussed in the previous two subsections (see Table 8 for the summary). The difference in Gibbs free energy for the gas phase in the direct mechanism obtained at the MP2/aug-cc-pVDZ level is ΔG(B→A) = −1.38 kcal/mol. The corresponding value of pK_a, using eq 7, calculated for this mechanism is pK_a = 1.0. This is quite underestimated compared with the experimental result[14a] of pK_a = 7.9 showing that the water environment plays a very important role in the tautomeric reaction of pterin. The calculated pK_a, values using the two reaction mechanisms in the gas phase and in aqueous environment are all presented in Table 8. Considering now the participation of one water molecule in the water-assisted mechanism added to the bulk effect of the aqueous solution, the difference in the Gibbs free energy is ΔG_{solv}(BW→AW) = −11.21 kcal/mol and the value of pK_a is calculated to be 8.2 (with an statistical error estimated as 0.6) in very good agreement with the experimental value. We thus verify that the water-assisted mechanism represents very well the qualitative and quantitative chemical process of the tautomeric equilibrium

of the pterin molecule in water. Changing the QM method, other values of the pK_a were calculated; we obtained pK_a = 8.8 with B3LYP/6-31+G(d,p) and 8.5 with PBE/6-31+G(d,p). These values are also in good agreement with experiment and with our best value of the pK_a (8.2 ± 0.6 kcal/mol) obtained with MP2/aug-cc-pVDZ.

4. Conclusions

The proton transfer reaction involved in the two tautomeric forms of pterin was studied in the gas phase and in aqueous solution using ab initio quantum mechanics and free energy perturbation implemented in Monte Carlo simulations. For this, a convenient nonphysical thermodynamic cycle is used. Two distinct reaction mechanisms were considered in this work, a direct intramolecular proton transfer and a solvent-assisted mechanism. In the gas phase, the intramolecular reaction mechanism at the MP2/aug-cc-pVDZ level leads to an energy barrier of 34.19 kcal/mol, passing through a three-center transition state. The tautomeric reaction assisted with one water molecule decreased the energy barrier to 10.37 kcal/mol, an impressive reduction of nearly 70% in comparison with the direct mechanism. Thus the water-assisted mechanism is crucial for obtaining a realistic barrier even not considering the bulk effect of the water environment. The situation is even clearer when considering the aqueous environment in room temperature. In this case using the direct mechanism the calculated free energy of solvation of ca. −16.4 kcal/mol is not sufficient to accurately determine the equilibrium constant and pK_a, even though it includes solvent effect. The result is a high value of pK_a of 12.0. The calculation of the free energy considering the water-assisted mechanism in the aqueous environment gives instead the result of 8.2 ± 0.6, which is in excellent agreement with the experimental result of 7.9. The theoretical results for the Gibbs free energy obtained here properly obtain the relative stability of the acid tautomer in agreement with the experimental results and quantitatively represent very well the experimental data.

Acknowledgment. P.J. is grateful to FAPESP for a postdoctoral fellowship. This work has been partially supported by the Brazilian agencies CNPq, CAPES, and FAPESP.

References and Notes

(1) Reichardt, C. *Solvent and Solvent Effects in Organic Chemistry*, 3rd ed.; Wiley-VCH: Weinheim, 2003.

(2) Mennucci, B., Cammi, R., Eds.; *Continuum Solvation Models in Chemical Physics*; Wiley: New York, 2007.

(3) Canuto, S., Eds.; *Solvation Effects on Molecules and Biomolecules. Computational Methods and Applications*; Springer: New York, 2008.

(4) (a) Blair, J. T.; Krogh-Jespersen, K.; Levy, R. M. *J. Am. Chem. Soc.* **1989**, *111*, 6948. (b) Gao, J. *J. Am. Chem. Soc.* **1994**, *116*, 9324. (c) Gao, J. L. In *Reviews of Computational Chemistry*; Lipkowitz, K. B., Boyd, D. B., Eds.; New York, 1996; Vol. 7, p 119. (d) Kongsted, J.; Osted, A.; Mikkelsen, K.; Christiansen, O. *J. Chem. Phys.* **2003**, *119*, 10519. (e) Miertus, S.; Scrocco, E.; Tomasi, J. *Chem. Phys.* **1981**, *55*, 117. (f) Mennucci, B.; Martinez, J. M.; Tomasi, J. *J. Phys. Chem. A* **2001**, *105*, 7287. (g) Tomasi, J.; Persico, M. *Chem. Rev.* **1994**, *94*, 2027. (h) Tomasi, J. *Theor. Chem. Acc.* **2004**, *112*, 184. (i) Coutinho, K.; Canuto, S. *J. Chem. Phys.* **2000**, *113*, 9132. (j) Canuto, S.; Coutinho, K.; Trzesniak, D. *Adv. Quantum Chem.* **2002**, *41*, 161. (k) Mikkelsen, K.; V.; Ågren, H.; Jensen, H. J. A.; Helgaker, T. *J. Chem. Phys.* **1988**, *89*, 3086. (l) Orozco, M.; Luque, F. J. *Chem. Rev.* **2000**, *100*, 4187. (m) Öhrn, A.; Karlström, G. *Mol. Phys.* **2006**, *104*, 3087. (n) Sánchez, M. L.; Aguilar, M. A.; Olivares Del Valle, F. J. *J. Comput. Chem.* **1997**, *18*, 313. (o) Ten-no, S.; Hirata, F.; Kato, S. *J. Chem. Phys.* **1994**, *100*, 7443. (p) Zeng, J.; Craw, J. S.; Hush, N. S.; Reimers, J. R. *J. Phys. Chem.* **1993**, *98*, 11075. (q) Klamt, A.; Schüürmann, G. *J. Chem. Soc., Perkins Trans.* **1993**, *2*, 799. (r) Monte, S. A.; Muller, T.; Dallos, M.; Lischka, H.; Diedenhofen, M.; Klamt, A. *Theor. Chem. Acc.* **2004**, *111*, 78. (s) Aquino, A. J. A.; Tunega, D.; Haberhauer, G.; Gerzabek, M. H.; Lischka, H. *J. Phys. Chem. A* **2002**, *106*, 1862.

(5) (a) Agmon, N. *Chem. Phys. Lett.* **1995**, *244*, 456. (b) Geiddler, P. L.; Dellago, C.; Chandler, D.; Hutter, J.; Parrinello, M. *Science* **2001**, *291*, 2121. (c) Tanner, C.; Manca, C.; Leutwyler, S. *Science* **2003**, *302*, 1736. (d) Mohammed, O. F.; Pines, D.; Dreyer, J.; Pines, E.; Nibbering, E. T. J. *Science* **2005**, *310*, 83. (e) Kamachi, T.; Yoshizawa, K. *J. Am. Chem. Soc.* **2005**, *127*, 10686. (f) Riccardi, D.; Knig, P.; Prat-Resina, X.; Yu, H.; Elstner, M.; Frauenhein, T.; Cui, Q. *J. Am. Chem. Soc.* **2006**, *128*, 16302. (g) Lima, M. C.; Coutinho, K.; Canuto, S.; Rocha, W. R. *J. Phys. Chem. A* **2006**, *110*, 7253.

(6) (a) Ando, K.; Hynes, J. T. *Adv. Chem. Phys.* **1999**, *110*, 381. (b) Schultz, B. E.; Chan, S. I. *Annu. Rev. Biophys. Biomol. Struct.* **2001**, *30*, 23. (c) Roux, B. *Acc. Chem. Res.* **2002**, *35*, 366. (d) Luecke, H.; Lanyi, J. K. *Adv. Protein Chem.* **2003**, *63*, 111. (e) Braun-Sand, S.; Strajbl, M.; Warshel, A. *Biophys. J.* **2004**, *87*, 2221. (f) Voth, G. A. *Acc. Chem. Res.* **2006**, *39*, 143.

(7) (a) Nichol, C. A.; Smith, G. K.; Duch, D. S. *Annu. Rev. Biochem.* **1985**, *62*, 729. (b) Hopkins, G. *Chemistry and Biology of Pteridines and Folates*; Ayling, J. E., Nair, M. G.,Baugh, C. M., Eds.; Plenum Press: New York, 1993. (c) Fuller, R. C.; Nugent, N. A. *Proc. Natl. Acad. Sci. U.S.A.* **1969**, *63*, 1311.

(8) Pirie, A.; Simpson, D. M. *Biochem. J.* **1946**, *40*, 14.

(9) Wijnen, B.; Leertouwer, H. L.; Stavenga, D. G. *J. Insect. Physiol.* **2007**, *53*, 1206.

(10) Galland, P.; Senger, H. *Photochem. Photobiol.* **1988**, *48*, 811.

(11) Hohl, N.; Galland, P.; Senger, H. *Photochem. Photobiol.* **1992**, *55*, 239.

(12) (a) Ito, K.; Kawanishi, S. *Biochemistry.* **1997**, *36*, 1774. (b) Lorente, C.; Thomas, A. H.; Villata, L. S.; Hozbor, D.; Lagares, A.; Capparelli, A. L. *Pteridines* **2000**, *11*, 100.

(13) (a) Thomas, A. H.; Lorente, C.; Capparelli, A. L.; Martínez, C. G.; Braun, A. M.; Oliveros, E. *Photochem. Photobiol. Sci.* **2003**, *2*, 245. (b) Cabrerizo, F. M.; Dántola, M. L.; Petroselli, G.; Capparelli, A. L.; Thomas, A. H.; Braun, A. M.; Lorente, C.; Oliveros, E. *Photochem. Photobiol.* **2007**, *83*, 526.

(14) (a) Thomas, A. H.; Lorente, C.; Capparelli, A. L.; Pokhrel, M. R.; Braun, A. M.; Oliveros, E. *Photochem. Photobiol. Sci.* **2002**, *1*, 421. (b) Lorente, C.; Thomas, A. H. *Acc. Chem. Res.* **2006**, *39*, 395.

(15) Cabrerizo, F. M.; Petroselli, G.; Lorente, C.; Capparelli, A. L.; Thomas, A. H.; Braun, A. M.; Oliveros, E. *Photochem. Photobiol.* **2005**, *81*, 1234.

(16) (a) Osdene, T. S.; Taylor, E. S. *J. Am. Chem. Soc.* **1956**, *78*, 5451. (b) Taylor, E. S.; Ray, P. S. *J. Org. Chem.* **1987**, *52*, 3997. (c) Heizmann, G.; Pfleiderer, W. *Helv. Chim. Acta* **2007**, *90*, 1856.

(17) Benkovic, S. J.; Sammons, D.; Armarego, W. L.; Waring, P.; Inners, R. *J. Am. Chem. Soc.* **1985**, *107*, 3706.

(18) (a) Gready, J. E. *J. Mol. Struct. (Theochem)* **1984**, *109*, 231. (b) Gready, J. E. *J. Mol. Struct. (Theochem)* **1985**, *124*, 1.

(19) Gready, J. E. *J. Am. Chem. Soc.* **1985**, *107*, 6689.

(20) Greatbanks, S. P.; Hillier, I. H.; Garner, C. D.; Joule, J. A. *J. Chem. Soc., Perkin Trans.* **1997**, *2*, 1529.

(21) Schwalbe, C. H.; Lowis, D. R.; Richards, W. G. *J. Chem. Soc., Chem. Commun.* **1993**, 1199.

(22) Schormann, N.; Senkovich, O.; Ananthan, S.; Chattopadhyay, D. *J. Mol. Struct. (Theochem)* **2003**, *635*, 37.

(23) Chen, X.; Xu, X.; Cao, Z. *J. Phys. Chem. A.* **2007**, *111*, 9255.

(24) Minkin, V. I.; Olekhnovich, L. P.; Zhdanov, Y. A. *Acc. Chem. Res.* **1981**, *14*, 210.

(25) (a) Alemán, C. *Chem. Phys.* **2000**, *253*, 13. (b) Remko, M.; Van Duijnen, P. Th.; Swart, M. *Struct. Chem.* **2003**, *14*, 271. (c) Xue, Y.; Kim, C. K.; Guo, Y.; Xie, D. Q.; Yan, G. S. *J. Comput. Chem.* **2005**, *26*, 994. (d) Gerega, A.; Lapinski, L.; Nowak, M. J.; Rostkowska, H. *J. Phys. Chem. A.* **2006**, *110*, 10244. (e) Mazzuca, D.; Marino, T.; Russo, N.; Toscano, M. *THEOCHEM.* **2007**, *811*, 161. (f) Lie, M. A.; Schiøtt, B. *J. Comput. Chem.* **2008**, *29*, 1037.

(26) (a) Zwanzig, R. W. *J. Chem. Phys.* **1954**, *22*, 1420. (b) Pearlman, D. A.; Rao, B. G.; *Encyclopedia of Computational Chemistry*; Schleyer, P. R., Ed.; John Wiley: Chichester, 1998; Vol. 2, p 1036; (c) Jorgensen, W. L.; *Encyclopedia of Computational Chemistry*; Schleyer, P. R., Ed.; John Wiley: Chichester, 1998; Vol. 2, p 1061; (d) Mark, A. E.; *Encyclopedia of Computational Chemistry*; Schleyer, P. R., Ed.; John Wiley: Chichester, 1998; Vol. 2, p 1070; (e) Straatsma; *Encyclopedia of Computational Chemistry*; Schleyer, P. R., Ed.; John Wiley: Chichester, 1998; Vol. 2, p 1083.

(27) (a) Becke, A. D. *J. Chem. Phys.* **1993**, *98*, 5648. (b) Lee., C.; Yang, W.; Parr, R. G. *Phys. Rev. B* **1988**, *37*, 785.

(28) Perdew, J. P.; Burke, K.; Ernzerhof, M. *Phys. Rev. Lett.* **1996**, *77*, 3865.

(29) (a) Ragavachari, K. *Annu. Rev. Phys. Chem.* **1991**, *42*, 615. (b) Bartlett, R. J.; Musial, M. *Rev. Mod. Phys.* **2007**, *79*, 291.

(30) (a) Onsager, L. *J. Am. Chem. Soc.* **1936**, *58*, 1486. (b) Wong, M. W.; Frisch, M. J.; Wiberg, K. B. *J. Am. Chem. Soc.* **1991**, *113*, 4776. (c) Wong, M. W.; Wiberg, K. B.; Frisch, M. J. *J. Chem. Phys.* **1991**, *95*, 8991. (d) Wong, M. W.; Wiberg, K. B.; Frisch, M. J. *J. Am. Chem. Soc.* **1992**, *114*,

523. (e) Wong, M. W.; Wiberg, K. B.; Frisch, M. J. *J. Am. Chem. Soc.* **1992**, *114*, 1645.

(31) Frisch, M. J.; Trucks, G. W.; Schlegel, H. B.; Scuseria, G. E.; Robb, M. A.; Cheeseman, J. R.; Montgomery, J. A., Jr.; Vreven, T.; Kudin, K. N.; Burant, J. C.; Millam, J. M.; Iyengar, S. S.; Tomasi, J.; Barone, V.; Mennucci, B.; Cossi, M.; Scalmani, G.; Rega, N.; Petersson, G. A.; Nakatsuji, H.; Hada, M.; Ehara, M.; Toyota, K.; Fukuda, R.; Hasegawa, J.; Ishida, M.; Nakajima, T.; Honda, Y.; Kitao, O.; Nakai, H.; Klene, M.; Li, X.; Knox, J. E.; Hratchian, H. P.; Cross, J. B.; Bakken, V.; Adamo, C.; Jaramillo, J.; Gomperts, R.; Stratmann, R. E.; Yazyev, O.; Austin, A. J.; Cammi, R.; Pomelli, C.; Ochterski, J. W.; Ayala, P. Y.; Morokuma, K.; Voth, G. A.; Salvador, P.; Dannenberg, J. J.; Zakrzewski, V. G.; Dapprich, S.; Daniels, A. D.; Strain, M. C.; Farkas, O.; Malick, D. K.; Rabuck, A. D.; Raghavachari, K.; Foresman, J. B.; Ortiz, J. V.; Cui, Q.; Baboul, A. G.; Clifford, S.; Cioslowski, J.; Stefanov, B. B.; Liu, G.; Liashenko, A.; Piskorz, P.; Komaromi, I.; Martin, R. L.; Fox, D. J.; Keith, T.; Al-Laham, M. A.; Peng, C. Y.; Nanayakkara, A.; Challacombe, M.; Gill, P. M. W.; Johnson, B.; Chen, W.; Wong, M. W.; Gonzalez, C.; Pople, J. A. *Gaussian 03*, revision C.02; Gaussian, Inc.: Wallingford, CT, 2004.

(32) Allen, M. P.; Tildesley, D. J. *Computer Simulation of Liquids*; Clarendon Press: Oxford, 1989.

(33) Berendsen, H. J. C.; Grigera, J. R.; Straatsma, T. P. *J. Phys. Chem.* **1987**, *91*, 6269.

(34) Jorgensen, W. L.; Maxwell, D. S.; Tirado-Rives, J. *J. Am. Chem. Soc.* **1996**, *118*, 11225.

(35) (a) Georg, H. C.; Coutinho, K.; Canuto, S. *Chem. Phys. Lett.* **2006**, *429*, 119. (b) Georg, H. C.; Coutinho, K.; Canuto, S. *J. Chem. Phys.* **2007**, *126*, 34507.

(36) (a) Coutinho, K.; Georg, H. C.; Fonseca, T. L.; Ludwig, V.; Canuto, S. *Chem. Phys. Lett.* **2007**, *437*, 148. (b) Sanchez, M. L.; Aguilar, M. A.; Olivares Del Valle, F. J. *J. Comput. Chem.* **1997**, *18*, 313.

(37) (a) Jorgensen, W. L.; Ravimohan, C. *J. Chem. Phys.* **1985**, *83*, 3050. (b) Jorgensen, W. L. *Acc. Chem. Res.* **1989**, *22*, 184. (c) Jorgensen, W. L.; Thomas, L. L. *J. Chem. Theory Comput.* **2008**, *4*, 869. (d) Georg, H. C.; Coutinho, K.; Canuto, S. *Chem. Phys. Lett.* **2005**, *413*, 16.

(38) Coutinho, K.; Canuto, S. *DICE: A Monte Carlo program for molecular liquid simulation*; University of São Paulo: Brazil, 2003.

(39) (a) Hamor, T. A.; Robertson, J. M. *J. Chem. Soc.* **1956**, 3586. (b) Shirrel, C. D.; Williams, D. E. *J. Chem. Soc., Perkin Trans.* **1975**, *2*, 40.

(40) (a) Aidas, K.; Kongsted, J.; Osted, A.; Mikkelsen, K. V.; Christiansen, O. *J. Phys. Chem. A.* **2005**, *109*, 8001. (b) Naka, K.; Morita, A.; Kato, S. *J. Chem. Phys.* **1999**, *111*, 481. (c) Illingworth, C. J. R.; Gooding, S. R.; Winn, P. J.; Jones, G. A.; Ferenczy, G. G.; Reynolds, C. A. *J. Phys. Chem. A* **2006**, *110*, 6487. (d) Gao, J.; Xia, X. *Science* **1992**, *258*, 631.

JP903638N